 CMES, vol.79, no.1, pp.1-29, 2011

Three Dimensional Acoustic Shape Sensitivity Analysis by Means of Adjoint Variable Method and Fast Multipole Boundary Element Approach

C.J. Zheng[1], H.B. Chen[1], T. Matsumoto[2] and T. Takahashi[2]

Abstract: A fast multipole boundary element approach to the shape sensitivity analysis of three dimensional acoustic wave problems is developed in this study based on the adjoint variable method. The concept of material derivative is employed in the derivation. The Burton-Miller formula which is a linear combination of the conventional and normal derivative boundary integral equations is adopted to cope with the non-uniqueness problem when solving exterior acoustic wave problems. Constant elements are used to discretize the boundary surface so that the strongly- and hyper-singular boundary integrals contained in the formulations can be evaluated explicitly and the numerical process can be performed efficiently. Numerical examples are given to demonstrate the accuracy and efficiency of the present algorithm.

Keywords: Acoustic shape sensitivity analysis, adjoint variable method, boundary element method, fast multipole method, Burton-Miller formula.

1 Introduction

The boundary element method (BEM), which emerged as a powerful alternative to the finite element method (FEM), has been widely applied to the acoustic prediction problems as it involves only surface discretization and solves exterior problems naturally. In many engineering applications, however, the prediction of the acoustic field using a technique such as the BEM constitutes only one step of an analysis process. It is often required to search for a configuration which can optimize the acoustic performance of the structure under consideration. In the shape optimization, we usually measure the acoustic performance using certain objective functions

[1] Department of Modern Mechanics, University of Science and Technology of China, Hefei, Anhui 230027, P.R.China

[2] Department of Mechanical Science and Engineering, Nagoya University, Furo-cho, Chikusa-ku, Nagoya 464-8604, Japan

and then attempt to find the extrema of these functions by changing the shape of the structure. The usual shape optimization algorithms can be classified into the gradient-based and gradient-free methods. In many cases the gradient-based methods are more efficient than the gradient-free methods if we can calculate the sensitivities of the objective functions efficiently [Udawalpola (2010)]. However, the calculation of sensitivities is usually very time-consuming and the accuracy of the evaluated sensitivities to a great extent affect the convergence of the gradient-based methods. Thus, the most crucial step in the gradient-based methods is to calculate the sensitivities of the objective functions accurately and efficiently.

Traditionally, the sensitivity formulations can be classified into two approaches: the direct differentiation method and the adjoint variable method [Kim and Dong (2006)]. The former calculates the sensitivities of state variables, e.g., by a sensitivity boundary integral equation, and then utilizes the chain rule of differentiation to evaluate the sensitivities of the objective functions. The latter, however, avoids calculating the sensitivities of state variables by introducing some adjoint problems. As for the acoustic boundary element sensitivity analysis discussed in this paper, the basic idea of the adjoint variable method is to avoid calculating the unknown sensitivity of sound pressure or particle velocity on the boundary or within the domain, as it needs to be calculated for each design variable in the direct differentiation method. As the computational cost of adjoint variable method does not depend on the number of design variables but on the number of objective functions, the adjoint variable method is often advantageous to use when there are large number of design variables, but relatively few objective functions [Udawalpola (2010)].

Much work has been presented for the acoustic boundary element shape sensitivity analysis based on the direct differentiation method. For instance, Smith and Bernhard (1992) proposed a semi-analytical boundary element sensitivity approach and resolved the well-known non-uniqueness problem by using the CHIEF method [Schenck (1968)]. Matsumoto, Tanaka, and Yamada (1995) and Koo, Ih, and Lee (1998) presented two different analytical sensitivity boundary integral equations with respect to the shape design variables. Arai, Tanaka, and Matsumoto (2007b) derived an analytical shape sensitivity equation based on a modified Burton-Miller formula [Arai, Tanaka, and Matsumoto (2007a)]. However, compared with the direct differentiation method, there are fewer publications on the adjoint variable method in the field of acoustic shape sensitivity analysis. Kim and Dong (2006) proposed a shape design sensitivity method for structural-acoustic problems based on sequential finite element and boundary element methods, where they obtained the adjoint equations directly from the discretized Helmholtz integral equation. Thus, their method can be termed as a discrete adjoint variable method, where the sensitivity of the coefficient matrix of the discretized Helmholtz integral equa-

tion is still required. Zhang, Bi, Chen, and Chen (2009) developed another adjoint variable method for structural-acoustic sensitivity analyses based on a wave superposition approach, but not the BEM, so as to eliminate the restrictions in the BEM such as singular integrals. Udawalpola, Wadbro, and Berggren (2011) presented an algorithm to optimize a variable mouth acoustic horn where the adjoint variable method is employed to provide the sensitivities.

The most distinctive feature of the BEM is that it only requires discretization of the surface rather than the volume, so that the BEM seems more efficient than domain methods such as the FEM at first glance. However, the conventional BEM produces a full and non-symmetric coefficient matrix which leads to increased computational cost in comparison with domain methods. This well-known obstacle had stood in the way of BEM for large-scale applications for several decades. As for a problem with N degrees of freedom, a direct solver such as the Gauss elimination requires the storage of $O(N^2)$ and the cost of $O(N^3)$. Use of iterative solvers, such as the GMRES [Saad and Schultz (1986)], does not reduce the storage requirements but can reduce the cost to $O(MN^2)$, where M is the number of iterations and $O(N^2)$ per iteration cost arising from the full matrix-vector product. This is still quite expensive for large-scale problems. In order to further improve the efficiency and reduce the storage requirements of the BEM with iterative solvers, various acceleration techniques, such as the fast multipole method (FMM) [Greengard and Rokhlin (1987)], the fast wavelet transforms [Beylkin, Coifman, and Rokhlin (1991)], the precorrected-FFT [Phillips and White (1997)] and the H-matrices [Hackbusch (1999)], have been proposed to accelerate the matrix-vector product. Among these methods, the FMM seems to be the most widely accepted methods in the fast BEM community. Moreover, it has also been acclaimed as one of the top ten algorithms of the 20th century [Cipra (2000)]. It allows the matrix-vector product to be performed in $O(N)$ operations and reduces the storage requirements to $O(N)$ as well, for instance, for potential problems or low-frequency acoustic problems [Nishimura (2002)]. It was first introduced by Greengard and Rokhlin [Greengard and Rokhlin (1987)] and then intensively studied and extended to the solution of problems arising from the Laplace, Helmholtz, Maxwell, and other equations [Coifman, Rokhlin, and Wandzura (1993); Rokhlin (1993); Epton and Dembart (1995); Rahola (1996); Greengard and Rokhlin (1997); Song, Lu, and Chew (1997); Gyure and Stalzer (1998); Cheng, Greengard, and Rokhlin (1999); Yoshida, Nishimura, and Kobayashi (2001); Darve and Havé (2004); Cheng, Crutchfield, Gimbutas, Greengard, Ethridge, Huang, Rokhlin, Yarvin, and Zhao (2006); Shen and Liu (2007a,b); Otani and Nishimura (2008); Gumerov and Duraiswami (2009); Wolf and Lele (2010)]. A comprehensive review can be found in [Nishimura (2002)].

This paper proposes a large-scale shape sensitivity analysis algorithm for three dimensional acoustic wave problems using the adjoint variable technique and the fast multipole boundary element approach. The concept of material derivative [Haug, Choi, and Komkov (1986)] is employed in the derivation, and the adjoint equations are derived in continuous forms so that the sensitivity of the coefficient matrix of the discretized Helmholtz integral equation is not required. The Burton-Miller formula [Burton and Miller (1971)] is used to tackle the non-uniqueness problem when solving exterior acoustic wave problems. Although the normal derivative boundary integral equation (NDBIE) is a hypersingular type involving a double normal derivative of the fundamental solution, such hypersingular terms can be evaluated explicitly and directly when constant elements are employed to discretize the boundary [Matsumoto, Zheng, Harada, and Takahashi (2010)].

2 Formulations

The propagation of time-harmonic acoustic waves in a homogeneous and isotropic acoustic medium can be described by the following Helmholtz equation:

$$\nabla^2 u(x) + k^2 u(x) = 0, \quad x \in \Omega \tag{1}$$

where ∇^2 is the Laplace operator, $u(x)$ the sound pressure at x, $k = \omega/c$ the wave number, ω the angular frequency, c the sound speed and Ω the infinite domain exterior to or the finite domain interior to a closed surface Γ.

Boundary conditions on Γ ($\Gamma = \Gamma_u + \Gamma_q + \Gamma_z$) are given as

$$u(x) = \bar{u}(x), \quad \text{on } \Gamma_u \tag{2}$$

$$q(x) = \frac{\partial u}{\partial n}(x) = \mathrm{i}\rho\omega\bar{v}(x), \quad \text{on } \Gamma_q \tag{3}$$

$$u(x) = zv(x), \quad \text{on } \Gamma_z \tag{4}$$

where $n(x)$ denotes the unit outward normal to the boundary at x, i the imaginary unit, ρ the density of the medium, $v(x)$ the normal velocity and z the acoustic impedance. The barred quantities indicate prescribed values on the boundary. As for exterior acoustic wave problems, the sound pressure at infinity must also satisfy the Sommerfeld radiation condition which ensures that all scattered and radiated waves are outgoing [Sommerfeld (1949)].

2.1 Acoustic boundary element analysis

The integral representation of the Helmholtz equation is

$$C(x)u(x) + \int\!\!\!\!\!\!-_{\Gamma} q^*(x,y)u(y)\,\mathrm{d}\Gamma(y) = \int_{\Gamma} u^*(x,y)q(y)\,\mathrm{d}\Gamma(y) \tag{5}$$

where x is the collocation point, y the source point. The symbol $\oint$ denotes that the integral is evaluated in the sense of Cauchy principal value. The coefficient $C(x) = 1,\ 1/2$ or 0 when x is inside the domain, on the smooth boundary or outside the domain. It should be noted that if Γ is not smooth at x, i.e., the tangent to Γ at x is non-unique, $C(x)$ has to be calculated specially [Ciskowski and Brebbia (1991)]. $u^*(x,y)$ is the fundamental solution, for three dimensional acoustic wave problems, given as

$$u^*(x,y) = \frac{\mathrm{e}^{\mathrm{i}kr}}{4\pi r}, \quad \text{with } r = |y-x| \tag{6}$$

and $q^*(x,y)$ is the normal derivative of $u^*(x,y)$, i.e.,

$$q^*(x,y) = -\frac{\mathrm{e}^{\mathrm{i}kr}}{4\pi r^2}(1-\mathrm{i}kr)\frac{\partial r}{\partial n(y)} \tag{7}$$

Eq. 5, usually referred to as the conventional boundary integral equation (CBIE), can be employed to calculate the unknown state values on the boundary. For instance, if the normal velocity is given on the boundary Γ, the sound pressure on Γ can be computed via Eq. 5. However, Eq. 5 does not always possess unique solutions for exterior acoustic wave problems [Schenck (1968)]. This is not a physical breakdown, but just arises from the drawback of the boundary integral equation for solving exterior wave propagation problems. Over the past decades, several strategies have been proposed to tackle this non-uniqueness problem. The combined Helmholtz integral equation formulation (CHIEF) presented by Schenck (1968) and the Burton-Miller formula proposed by Burton and Miller (1971) are by far the two most popular approaches. The Burton-Miller formula which is a linear combination of the CBIE and NDBIE, however, is more rigorous to conquer the non-uniqueness than the CHIEF, especially in the high frequency range [Amini and Harris (1990)]. Hence, the Burton-Miller formula is adopted in this study.

Taking the directional derivative of Eq. 5 in the direction $n(x)$ gives the following NDBIE:

$$C(x)q(x) + \oint\!\!\!\!\!\!= \int_\Gamma \tilde{q}^*(x,y)u(y)\,\mathrm{d}\Gamma(y) = \oint\!\!\!\!\!\!= \int_\Gamma \tilde{u}^*(x,y)q(y)\,\mathrm{d}\Gamma(y) \tag{8}$$

where the symbol $\oint\!\!\!\!\!\!=$ indicates that the integration is carried out in the sense of Hadamard finite part of the divergent integral, and $\tilde{(\,)} = \partial(\,)/\partial n(x)$, i.e.,

$$\tilde{u}^*(x,y) = -\frac{\mathrm{e}^{\mathrm{i}kr}}{4\pi r^2}(1-\mathrm{i}kr)\frac{\partial r}{\partial n(x)} \tag{9}$$

$$\tilde{q}^*(x,y) = \frac{\mathrm{e}^{\mathrm{i}kr}}{4\pi r^3}\left[(3-3\mathrm{i}kr-k^2r^2)\frac{\partial r}{\partial n(x)}\frac{\partial r}{\partial n(y)} + (1-\mathrm{i}kr)n_i(x)n_i(y)\right] \tag{10}$$

In Eq. 10, n_i is the cartesian component of the vector $n(x)$ or $n(y)$. Einstein's summation convention is used throughout the paper, so repeated indices imply summation over their range.

The linear combination of the CBIE and NDBIE can be written as

$$C(x)u(x)+\oint_\Gamma q^*(x,y)u(y)\,\mathrm{d}\Gamma(y)+\alpha\oint_\Gamma \tilde{q}^*(x,y)u(y)\,\mathrm{d}\Gamma(y)$$
$$=-\alpha C(x)q(x)+\int_\Gamma u^*(x,y)q(y)\,\mathrm{d}\Gamma(y)+\alpha\oint_\Gamma \tilde{u}^*(x,y)q(y)\,\mathrm{d}\Gamma(y) \tag{11}$$

where α is the coupling constant that can be chosen as i/k [Kress (1985)]. Usually, the above equation is referred to as the Burton-Miller formula.

Discretizing Eq. 11, collecting the equations for all collocation points and expressing them in matrix form result in the following linear algebraic equations:

$$[H]\{u\}=[G]\{q\} \tag{12}$$

Rearranging Eq. 12, that is moving all the unknown terms to the left-hand side and all the known terms to the right-hand side according to the boundary conditions, gives the following system of linear equations:

$$[A]\{\psi\}=[B]\{\phi\} \tag{13}$$

where $\{\psi\}$ and $\{\phi\}$ are the unknown and known vectors, respectively; $[A]$ and $[B]$ are the coefficient matrices corresponding to them. Eq. 13 can now be solved and all the unknown boundary state values are then obtained. Once this has been done, one can calculate the sound pressure $u(x)$ at any point x inside the domain by using Eq. 5 with the coefficient $C(x)=1$.

The strongly- and hyper-singular boundary integrals are found in Eq. 11. In order to evaluate them accurately, various singularity subtraction techniques have been proposed in the literature [Chien, Rajiyah, and Atluri (1990); Liu and Rizzo (1992); Tanaka, Sladek, and Sladek (1994); Hwang (1997); Yan, Hung, and Zheng (2003); Qian, Han, and Atluri (2004); Qian, Han, Ufimtsev, and Atluri (2004); Chen, Fu, and Zhang (2007); Li and Huang (2010)]. But most of these techniques are still cumbersome and sometimes time-consuming to use, especially in the FMBEM approach. For instance, when the formula is regularized by using the fundamental solution of Laplace's equation, multipole expansion formulas and other translation formulas have to be implemented not only for the fundamental solution and its derivatives of the Helmholtz equation but also for those of Laplace's equation. However, because constant elements are employed to discretize the boundary in this study, the strongly- and hyper-singular boundary integrals can be evaluated directly

and the derived formula is more efficient to use in the FMBEM. According to our previous work [Matsumoto, Zheng, Harada, and Takahashi (2010)], we have the non-singular version of Eq. 11 for the constant element discretization as follows:

$$\begin{aligned}
&\frac{1}{2}u(x)+\int_{\Gamma\backslash\Gamma_x} q^*(x,y)u(y)\,\mathrm{d}\Gamma(y)+\alpha\int_{\Gamma\backslash\Gamma_x}\tilde{q}^*(x,y)u(y)\,\mathrm{d}\Gamma(y)\\
&=-\frac{\alpha}{2}q(x)+\int_{\Gamma\backslash\Gamma_x} u^*(x,y)q(y)\,\mathrm{d}\Gamma(y)+\alpha\int_{\Gamma\backslash\Gamma_x}\tilde{u}^*(x,y)q(y)\,\mathrm{d}\Gamma(y)\\
&+\frac{\mathrm{i}}{2k}\left(1-\int_0^{2\pi}\frac{\mathrm{e}^{\mathrm{i}kR}}{2\pi}\,\mathrm{d}\theta\right)q(x)-\alpha\left(\frac{\mathrm{i}k}{2}-\int_0^{2\pi}\frac{\mathrm{e}^{\mathrm{i}kR}}{4\pi R}\,\mathrm{d}\theta\right)u(x)
\end{aligned}\tag{14}$$

where $\Gamma\backslash\Gamma_x$ denotes the boundary Γ excluding Γ_x the element in which the collocation point x exists, $R=R(\theta)$ the distance from x to the peripheral of the elment.

2.2 Acoustic shape sensitivity analysis

The main purpose of this study is to evaluate the first-order sensitivity of an acoustic objective function accurately and efficiently. Without loss of generality, we define the objective function J in an arbitrary form as follows:

$$J=\int_\Gamma g(u,q)\,\mathrm{d}\Gamma+\int_\Omega h(u)\,\mathrm{d}\Omega \tag{15}$$

where g is a function of sound pressure and its normal derivative on the boundary, and h a function of sound pressure inside the domain.

The first-order sensitivity of the objective function can be obtained by taking the material derivative of Eq. 15 with respect to an arbitrary design variable as follows:

$$\dot{J}=\int_\Gamma \dot{g}(u,q)\,\mathrm{d}\Gamma+\int_\Gamma g(u,q)\,\mathrm{d}\dot{\Gamma}+\int_\Omega \dot{h}(u)\,\mathrm{d}\Omega+\int_\Omega h(u)\,\mathrm{d}\dot{\Omega} \tag{16}$$

where the upper dot $\dot{()}$ denotes the material derivative with respect to the design variable. According to [Haug, Choi, and Komkov (1986); Arora (1993); Burczyński, Kane, and Balakrishna (1995)], the total material derivatives of the surface and domain element are respectively given by

$$\mathrm{d}\dot{\Gamma}=(\dot{x}_{i,i}-\dot{x}_{i,j}n_in_j)\,\mathrm{d}\Gamma \tag{17}$$

$$\mathrm{d}\dot{\Omega}=\dot{x}_{i,i}\,\mathrm{d}\Omega \tag{18}$$

where an index after a comma denotes the partial derivative with respect to the coordinate component, e.g., $\dot{x}_{i,j}=\partial\dot{x}_i/\partial x_j$.

Furthermore, the material derivatives of g and h can be obtained by the chain rule of differentiation as follows:

$$\dot{g}(u,q) = \frac{\partial g}{\partial u}\dot{u} + \frac{\partial g}{\partial q}\dot{q} \tag{19}$$

$$\dot{h}(u) = \frac{\partial h}{\partial u}\dot{u} \tag{20}$$

Thus, in order to evaluate $\dot{J}$, it seems essential to know all values of $\dot{u}$ and $\dot{q}$ on the boundary and also $\dot{u}$ at any desired part within the domain. The unknown sensitivity values of state variables can be calculated in the direct differentiation method. However, since an additional boundary value problem for each design variable is required in the direct differentiation method, when the number of design variables is larger than that of objective functions, the direct differentiation method is found to be less efficient than the adjoint variable method [Udawalpola (2010)]. In the adjoint variable method, the unknown values of $\dot{u}$ and $\dot{q}$ are eliminated from the sensitivity equations of the objective functions by introducing certain adjoint problems corresponding to the objective functions, but not the design variables. Theoretical fundamentals of the adjoint variable method have been well presented by Haug, Choi, and Komkov (1986).

In order to eliminate the unknown sensitivities of state variables in the sensitivity equation of J, a constraint condition is added to the objective function J to form an augmented function as follows:

$$\hat{J} = J + R = \int_\Gamma g(u,q)\,\mathrm{d}\Gamma + \int_\Omega h(u)\,\mathrm{d}\Omega + \int_\Omega \lambda(x)[\nabla^2 u(x) + k^2 u(x)]\,\mathrm{d}\Omega \tag{21}$$

Because the equation $\nabla^2 u(x) + k^2 u(x) = 0$ is always satisfied within the domain Ω, the added term does not have any affection to the original function J, i.e., $\hat{J}$ is actually identical to J. According to the derivation presented in the appendix, we obtain the material derivative of $\hat{J}$ as follows:

$$\begin{aligned}
\dot{\hat{J}} = & \int_\Gamma \left(\frac{\partial g}{\partial u} - \frac{\partial \lambda}{\partial n}\right)\dot{u}\,\mathrm{d}\Gamma + \int_\Gamma \left(\frac{\partial g}{\partial q} + \lambda\right)\dot{q}\,\mathrm{d}\Gamma \\
& + \int_\Gamma \left(\lambda_{,j} q + \frac{\partial \lambda}{\partial n} u_{,j} - \lambda_{,i} u_{,i} n_j + k^2 \lambda u n_j\right)\dot{x}_j\,\mathrm{d}\Gamma \\
& + \int_\Gamma (g(u,q) + \lambda q)\,\mathrm{d}\dot{\Gamma} + \int_\Omega \left(\lambda_{,ii} + k^2\lambda + \frac{\partial h}{\partial u}\right)\dot{u}\,\mathrm{d}\Omega \\
& - \int_\Omega (\lambda_{,ii} + k^2\lambda) u_{,j}\dot{x}_j\,\mathrm{d}\Omega + \int_\Omega h(u)\,\mathrm{d}\dot{\Omega}
\end{aligned} \tag{22}$$

Then, if we define the adjoint equation as

$$\nabla^2\lambda(x)+k^2\lambda(x)+\frac{\partial h}{\partial u}=0, \quad x\in\Omega \tag{23}$$

with the following boundary conditions:

$$\frac{\partial\lambda}{\partial n}(x)=\frac{\partial g}{\partial u}, \quad x\in\Gamma_q \tag{24}$$

$$\lambda(x)=-\frac{\partial g}{\partial q}, \quad x\in\Gamma_u \tag{25}$$

Eq. 22 turns into

$$\begin{aligned}\dot{J}=&\int_{\Gamma_u}\left(\frac{\partial g}{\partial u}-\frac{\partial\lambda}{\partial n}\right)\dot{u}\,\mathrm{d}\Gamma+\int_{\Gamma_q}\left(\frac{\partial g}{\partial q}+\lambda\right)\dot{q}\,\mathrm{d}\Gamma\\&+\int_{\Gamma}\left(\lambda_{,j}q+\frac{\partial\lambda}{\partial n}u_{,j}-\lambda_{,i}u_{,i}n_j+k^2\lambda u n_j\right)\dot{x}_j\,\mathrm{d}\Gamma\\&+\int_{\Gamma}(g(u,q)+\lambda q)\,\mathrm{d}\dot{\Gamma}+\int_{\Omega}\frac{\partial h}{\partial p}u_{,j}\dot{x}_j\,\mathrm{d}\Omega+\int_{\Omega}h(u)\,\mathrm{d}\dot{\Omega}\end{aligned} \tag{26}$$

Also, we have

$$\int_{\Omega}\frac{\partial h}{\partial u}u_{,j}\dot{x}_j\,\mathrm{d}\Omega+\int_{\Omega}h(u)\,\mathrm{d}\dot{\Omega}=\int_{\Omega}\left(h\dot{x}_j\right)_{,j}\mathrm{d}\Omega=\int_{\Gamma}h\dot{x}_j n_j\,\mathrm{d}\Gamma \tag{27}$$

Substituting Eq. 27 into Eq. 26, and considering h defined within the domain Ω, we obtain

$$\begin{aligned}\dot{J}=&\int_{\Gamma_u}\left(\frac{\partial g}{\partial u}-\frac{\partial\lambda}{\partial n}\right)\dot{u}\,\mathrm{d}\Gamma+\int_{\Gamma_q}\left(\frac{\partial g}{\partial q}+\lambda\right)\dot{q}\,\mathrm{d}\Gamma\\&+\int_{\Gamma}\left(\lambda_{,j}q+\frac{\partial\lambda}{\partial n}u_{,j}-\lambda_{,i}u_{,i}n_j+k^2\lambda u n_j\right)\dot{x}_j\,\mathrm{d}\Gamma\\&+\int_{\Gamma}(g(u,q)+\lambda q)\,\mathrm{d}\dot{\Gamma}+\int_{\Gamma}h\dot{x}_j n_j\,\mathrm{d}\Gamma\end{aligned} \tag{28}$$

Finally, the unknown sensitivity values of state variables on the boundary and within the domain are eliminated from Eq. 28 to compute the sensitivity of the objective function. However, it is noted that the boundary gradients of sound pressure u and adjoint solution λ are introduced in the above sensitivity equation. As the

BEM is employed in this study, the gradients for sound pressure can be calculated by the following boundary integral equation:

$$C(x)\frac{\partial u(x)}{\partial x_i}+\neq\!\!\!\!\int_{\Gamma}\frac{\partial q^*(x,y)}{\partial x_i}u(y)\,\mathrm{d}\Gamma=\int_{\Gamma}\frac{\partial u^*(x,y)}{\partial x_i}q(y)\,\mathrm{d}\Gamma \tag{29}$$

When the constant element discretization is used, we can obtain the non-singular version of Eq. 29 as follows:

$$\begin{aligned}&\frac{1}{2}\frac{\partial u(x)}{\partial x_i}+\int_{\Gamma\setminus\Gamma_x}\frac{\partial q^*(x,y)}{\partial x_i}u(y)\,\mathrm{d}\Gamma=\int_{\Gamma\setminus\Gamma_x}\frac{\partial u^*(x,y)}{\partial x_i}q(y)\,\mathrm{d}\Gamma\\&-\left(\frac{\mathrm{i}k}{2}-\int_0^{2\pi}\frac{\mathrm{e}^{\mathrm{i}kR}}{4\pi R}\,\mathrm{d}\theta\right)u(x)n_i(x)+\frac{1}{4\pi}q(x)\int_0^{2\pi}\frac{\partial r}{\partial y_i}(F(kR)-\mathrm{e}^{\mathrm{i}kR})\,\mathrm{d}\theta\end{aligned} \tag{30}$$

where $F(x)=\mathrm{Ci}(x)+\mathrm{iSi}(x)$, and $\mathrm{Ci}(x)$ and $\mathrm{Si}(x)$ are cosine and sine integrals defined as

$$\mathrm{Ci}(x)=-\int_x^{\infty}\frac{\cos t}{t}\,\mathrm{d}t \tag{31}$$

$$\mathrm{Si}(x)=\int_0^{x}\frac{\sin t}{t}\,\mathrm{d}t \tag{32}$$

From Eqs. 23, 24 and 25, it is noticed that the adjoint problem is analogous to the primary acoustic prediction problem, but with different boundary conditions and source term. So, the boundary integral equations and the solution procedures for the adjoint solution are very similar to those for acoustic state variables. Nevertheless, because of the source term contained in Eq. 23, we now need to carry out integrals in the domain as well as on the boundary when solving the boundary integral equations for adjoint solution. A great deal of research effort has been done to transform the domain integrals into equivalent boundary integrals so as to keep the "boundary only" nature of the BEM. The most important of these techniques are the Multiple Reciprocity Method [Nowak (1989)] and the Dual Reciprocity Method [Partridge, Brebbia, and Wrobel (1991)]. However, as the acoustic states at some separate observation points within the domain are usually used to represent the acoustic performance of the structure in the actual analysis, the source term consists of some concentrated sources which can be handled easily in the BEM [Brebbia and Dominguez (1989)]. Thus, we only present the formulations for the computation of acoustic state variables here, which can be extended easily to the calculation of the adjoint solution.

3 Wideband Fast Multipole Method

The formulations required in the wideband FMM approach are listed in this section. Although most of them can be found elsewhere [Rokhlin (1993); Epton and Dembart (1995); Rahola (1996); Yoshida (2001)], we present them below systematically in order to employ the wideband FMM approach in our acoustic shape sensitivity analysis.

The FMM approach to acoustic wave problems in the frequency domain consists of the low- and high-frequency strategies. The computational cost is proportional to N in the low-frequency FMM, versus to $N\log N$ in the high-frequency FMM. However, either of them fails in some way outside its preferred frequency region. The low-frequency FMM is found to be inefficient for high-frequency problems, while the high-frequency FMM is known to be unstable for low-frequency problems [Nishimura (2002)]. In each case, the difficulty is fundamental and cannot be overcome by simple expedients such as scaling, etc [Cheng, Greengard, and Rokhlin (1999)]. Thus, the wideband version which is accurate and efficient for any frequency seems necessary. It unifies the FMMs for low and high frequencies and switches between them depending on the level in the tree structure.

In order to apply the FMM approach, the fundamental solution of the Helmholtz equation should be expanded into a suitable form. The wideband FMM employed in this study uses a serious expansion formula of the fundamental solution in the low-frequency region and a plane wave expansion formula in the high-frequency region. In the low-frequency region, the fundamental solution is expanded into the following series around an expansion point O near y:

$$u^*(x,y) = \frac{\mathrm{i}k}{4\pi} \sum_{n=0}^{\infty} \sum_{m=-n}^{n} (2n+1) \bar{I}_n^m(k, \overrightarrow{Oy}) O_n^m(k, \overrightarrow{Ox}), \quad |\overrightarrow{Ox}| > |\overrightarrow{Oy}| \tag{33}$$

where I_n^m and O_n^m are defined as

$$I_n^m(k, \overrightarrow{a}) = j_n(kr) Y_n^m(\theta, \phi) \tag{34}$$

$$O_n^m(k, \overrightarrow{a}) = h_n^{(1)}(kr) Y_n^m(\theta, \phi) \tag{35}$$

and $\bar{I}_n^m$ is the complex conjugate of I_n^m, j_n and $h_n^{(1)}$ the n-th order spherical Bessel and Hankel functions of the first kind, Y_n^m the spherical harmonics defined as

$$Y_n^m(\theta, \phi) = \sqrt{\frac{(n-m)!}{(n+m)!}} P_n^m(\cos\theta) \, \mathrm{e}^{\mathrm{i}m\phi} \tag{36}$$

where P_n^m stand for the associated Legendre functions; r, θ and ϕ represent the three spherical coordinates of some vector $\overrightarrow{a}$, such as $\overrightarrow{Ox}$ or $\overrightarrow{Oy}$, for instance.

The plane wave expansion formula of the fundamental solution is written as follows:

$$u^*(x,y) = \frac{\mathrm{i}k}{16\pi^2} \int_S \mathrm{e}^{\mathrm{i}k\hat{\mathbf{k}}\cdot\overrightarrow{x'x}} T(k,\hat{\mathbf{k}},\overrightarrow{Ox'})\, \mathrm{e}^{-\mathrm{i}k\hat{\mathbf{k}}\cdot\overrightarrow{Oy}}\, \mathrm{d}S \tag{37}$$

where O and x' are points near y and x, the integration is taken over the unit sphere S, $\hat{\mathbf{k}}$ stands for the outward unit vector on S, and the diagonal translation function T is given by

$$T(k,\hat{\mathbf{k}},\overrightarrow{Ox'}) = \sum_{n=0}^{\infty} \mathrm{i}^n (2n+1) h_n^{(1)}(k|\overrightarrow{Ox'}|) P_n\left(\hat{\mathbf{k}}\cdot\frac{\overrightarrow{Ox'}}{|\overrightarrow{Ox'}|}\right) \tag{38}$$

where P_n denote the Legendre polynomials.

Using Eq. 33 and 37, one can write the boundary integrals over a boundary element Γ_j which is far away from the collocation point x as follows:

$$\left.\begin{matrix} H^{ij}u^j \\ G^{ij}q^j \end{matrix}\right\} = \frac{\mathrm{i}k}{4\pi} \sum_{n=0}^{\infty} \sum_{m=-n}^{n} (2n+1) M_n^m(k,\overrightarrow{Oy^j}) \left(O_n^m(k,\overrightarrow{Ox}) + \alpha \frac{\partial O_n^m(k,\overrightarrow{Ox})}{\partial n(x)} \right) \tag{39}$$

and

$$\left.\begin{matrix} H^{ij}u^j \\ G^{ij}q^j \end{matrix}\right\} = \frac{\mathrm{i}k}{16\pi^2} \int_S (1+\alpha \mathrm{i}k\hat{\mathbf{k}}\cdot n(x))\, \mathrm{e}^{\mathrm{i}k\hat{\mathbf{k}}\cdot\overrightarrow{x'x}} T(k,\hat{\mathbf{k}},\overrightarrow{Ox'})\, F(k,\hat{\mathbf{k}},\overrightarrow{Oy^j})\, \mathrm{d}S \tag{40}$$

where y^j is a source point on Γ_j; $M_n^m(k,\overrightarrow{Oy^j})$ and $F(k,\hat{\mathbf{k}},\overrightarrow{Oy^j})$, defined in the following, are multipole moments of low- and high-frequency FMM approaches, respectively.

$$M_n^m(k,\overrightarrow{Oy^j}) = \begin{cases} \displaystyle\int_{\Gamma_j} \frac{\partial \bar{I}_n^m(k,\overrightarrow{Oy})}{\partial n(y)} u^j \,\mathrm{d}\Gamma(y), & \text{for } H^{ij}u^j, \\ \displaystyle\int_{\Gamma_j} \bar{I}_n^m(k,\overrightarrow{Oy}) q^j \,\mathrm{d}\Gamma(y), & \text{for } G^{ij}q^j \end{cases} \tag{41}$$

and

$$F(k,\hat{\mathbf{k}},\overrightarrow{Oy^j}) = \begin{cases} \displaystyle\int_{\Gamma_j} -\mathrm{i}k\hat{\mathbf{k}}\cdot n(y)\, \mathrm{e}^{-\mathrm{i}k\hat{\mathbf{k}}\cdot\overrightarrow{Oy}} u^j \,\mathrm{d}\Gamma(y), & \text{for } H^{ij}u^j, \\ \displaystyle\int_{\Gamma_j} \mathrm{e}^{-\mathrm{i}k\hat{\mathbf{k}}\cdot\overrightarrow{Oy}} q^j \,\mathrm{d}\Gamma(y), & \text{for } G^{ij}q^j \end{cases} \tag{42}$$

Moments of a group of ℓ source elements that are close to O, exactly speaking, all elements in the same leaf cell defined in the next section and centered at O, can be added up together to form the moments of the leaf cell:

$$M_n^m(k,O) = \sum_{j=1}^{\ell} M_n^m(k,\overrightarrow{Oy^j}) \tag{43}$$

and

$$F(k,\hat{\mathbf{k}},O) = \sum_{j=1}^{\ell} F(k,\hat{\mathbf{k}},\overrightarrow{Oy^j}) \tag{44}$$

The M2M (Moments to Moments), M2L (Moments to Local expansion) and L2L (Local expansion to Local expansion) translation formulas for the low-frequency FMM approach are given as

$$\begin{aligned} M_n^m(k,O') = \sum_{n'=0}^{\infty} \sum_{m'=-n'}^{n'} \sum_{l\in\mathscr{L}(n,n',m,m')} & (2n'+1)(-1)^{m'} W_{n,n',m,m',l} \\ & \times I_l^{-m-m'}(k,\overrightarrow{O'O}) M_{n'}^{-m'}(k,O) \end{aligned} \tag{45}$$

$$\begin{aligned} L_n^m(k,x') = \sum_{n'=0}^{\infty} \sum_{m'=-n'}^{n'} \sum_{l\in\mathscr{L}(n,n',m,m')} & (2n'+1)(-1)^{m+m'} W_{n',n,m',m,l} \\ & \times O_l^{m+m'}(k,\overrightarrow{O'x'}) M_{n'}^{m'}(k,O') \end{aligned} \tag{46}$$

$$\begin{aligned} L_n^m(k,x'') = \sum_{n'=0}^{\infty} \sum_{m'=-n'}^{n'} \sum_{l\in\mathscr{L}(n,n',m,m')} & (2n'+1)(-1)^{m} W_{n',n,m',-m,l} \\ & \times I_l^{m-m'}(k,\overrightarrow{x'x''}) L_{n'}^{m'}(k,x') \end{aligned} \tag{47}$$

where $W_{n,n',m,m',l}$ is given by

$$W_{n,n',m,m',l} = (2l+1)\,\mathrm{i}^{n'-n+l} \begin{pmatrix} n & n' & l \\ 0 & 0 & 0 \end{pmatrix} \begin{pmatrix} n & n' & l \\ m & m' & -m-m' \end{pmatrix} \tag{48}$$

and $\begin{pmatrix} \cdots \\ \cdots \end{pmatrix}$ stands for the Wigner 3j symbol [Abramowitz and Stegun (1972)], and the set $\mathscr{L}$ is defined as

$$\mathscr{L}(n,n',m,m') = \{l \,|\, l\in\mathbb{Z},\, n+n'-l : \text{even},\, \max\{|m+m'|,|n-n'|\} \le l \le n+n'\} \tag{49}$$

The M2M, M2L and L2L translation formulas for the high-frequency FMM, denoted as F2F, F2H and H2H for distinguishing in this paper, are given by

$$F(k,\hat{\mathbf{k}},O') = \mathrm{e}^{-\mathrm{i}k\hat{\mathbf{k}}\cdot\overrightarrow{O'O}} F(k,\hat{\mathbf{k}},O) \tag{50}$$

$$H(k,\hat{\mathbf{k}},x') = T(k,\hat{\mathbf{k}},\overrightarrow{O'x'})F(k,\hat{\mathbf{k}},O') \tag{51}$$

$$H(k,\hat{\mathbf{k}},x'') = \mathrm{e}^{\mathrm{i}k\hat{\mathbf{k}}\cdot\overrightarrow{x'x''}} H(k,\hat{\mathbf{k}},x') \tag{52}$$

Finally, for the group of ℓ source elements that are close to O and far away from the collocation point x, $\sum_{j=1}^{\ell} H^{ij}u^j$ or $\sum_{j=1}^{\ell} G^{ij}q^j$ can be expressed in the form of expansion using the local expansion coefficients as

$$\sum_{j=1}^{\ell} H^{ij}u^j \text{ or } \sum_{j=1}^{\ell} G^{ij}q^j = \frac{\mathrm{i}k}{4\pi}\sum_{n=0}^{\infty}\sum_{m=-n}^{n}(2n+1)L_n^m(k,x'') \times\left(\bar{I}_n^m(k,\overrightarrow{x''x}) + \alpha\frac{\partial \bar{I}_n^m(k,\overrightarrow{x''x})}{\partial n(x)}\right) \tag{53}$$

in the low-frequency FMM, and

$$\sum_{j=1}^{\ell} H^{ij}u^j \text{ or } \sum_{j=1}^{\ell} G^{ij}q^j = \frac{\mathrm{i}k}{16\pi^2}\int_S (1+\alpha\mathrm{i}k\hat{\mathbf{k}}\cdot n(x))\,\mathrm{e}^{\mathrm{i}k\hat{\mathbf{k}}\cdot\overrightarrow{x''x}} H(k,\hat{\mathbf{k}},x'')\,\mathrm{d}S \tag{54}$$

in the high-frequency FMM.

Also, the boundary integrals for gradients can be written in the form of expansion using the local expansion coefficients as

$$\sum_{j=1}^{\ell} u^j\int_{\Gamma_j}\frac{\partial q^*}{\partial x_i}\mathrm{d}\Gamma \text{ or } \sum_{j=1}^{\ell} q^j\int_{\Gamma_j}\frac{\partial p^*}{\partial x_i}\mathrm{d}\Gamma = \frac{\mathrm{i}k}{4\pi}\sum_{n=0}^{\infty}\sum_{m=-n}^{n}(2n+1)L_n^m(k,x'')\frac{\partial \bar{I}_n^m(k,\overrightarrow{x''x})}{\partial x_i} \tag{55}$$

in the low-frequency FMM, and

$$\sum_{j=1}^{\ell} u^j\int_{\Gamma_j}\frac{\partial q^*}{\partial x_i}\mathrm{d}\Gamma \text{ or } \sum_{j=1}^{\ell} q^j\int_{\Gamma_j}\frac{\partial p^*}{\partial x_i}\mathrm{d}\Gamma = \frac{\mathrm{i}k}{16\pi^2}\int_S \mathrm{i}k\hat{\mathbf{k}}_i\,\mathrm{e}^{\mathrm{i}k\hat{\mathbf{k}}\cdot\overrightarrow{x''x}} H(k,\hat{\mathbf{k}},x'')\,\mathrm{d}S \tag{56}$$

in the high-frequency FMM.

In the wideband FMM, we use the following formula (M2F) to convert the low-frequency moments to the high-frequency moments:

$$F(k,\hat{\mathbf{k}},O)=\sum_{n=0}^{\infty}\sum_{m=-n}^{n}(2n+1)\,\mathrm{i}^{-n}Y_n^m(\hat{\mathbf{k}})M_n^m(k,O) \tag{57}$$

The local expansion coefficients of the high-frequency FMM can also be converted to those of the low-frequency FMM by using the following H2L formula:

$$L_n^m(k,x')=\frac{\mathrm{i}^n}{4\pi}\int_S Y_n^m(\hat{\mathbf{k}})H(k,\hat{\mathbf{k}},x')\,\mathrm{d}S \tag{58}$$

4 FMM algorithm

With all the formulas presented above, we are able to construct the wideband FMM algorithm for the three dimensional acoustic shape sensitivity analysis based on the adjoint variable method.

4.1 Preparation

Discretize the boundary surface Γ using boundary elements, for instance, constant triangular elements in the numerical examples of this paper. Consider a cube enclosing the whole domain as the cell of level 0, then divide this cell (a parent cell) into eight equal cubes and call any of the cubes a cell of level 1 (a child cell) if it contains boundary elements. Keep dividing a cell in this way until the number of elements in it is less than a specified number and call the childless cell a leaf cell.

Some terms are defined to make the following descriptions clearer. Two cells at level l are said to be *adjacent* if they share at least one vertex. If two cells are not adjacent at level l but their parent cells are adjacent at level $l-1$, they are said to be *well-separated*. The list of all well-separated cells of cell C forms the *interaction list of C*. Cells whose parent cells are not adjacent to the parent cell of C are called *far cells of C*. The switching level s between the low- and high-frequency FMM is the level which satisfies $d^{s+1}<D$ and $d^s\geq D$ (where d^s and d^{s+1} are the edge lengthes of cells at level s and $s+1$, and D the threshold between the low- and high-frequency FMM).

4.2 Upward pass

Calculate the moments of all cells down from level 2. As for a leaf cell C at level l, the moments are the summation of moments from all the boundary elements included in C to the center of C. If $l>s$, the low-frequency moments are needed, otherwise the high-frequency moments are needed. As for a non-leaf cell C at level

l, shift the moments from the center of its child cells to its center by the M2M translation if $l \geq s$, or the F2F translation if $l < s$, then add up all the translated moments together to form the moments of C. However, if $l = s$, the M2F conversion should be used after the M2M translation to convert the low-frequency moments to the high-frequency moments.

4.3 Downward pass

Calculate the local expansion coefficients of all cells at all levels with $l \geq 2$. The local expansion coefficients of cell C at level l consist of two parts. One is obtained from all cells in the interaction list of C by using the M2L translation if $l > s$ or the F2H translation if $l \leq s$; while, the other is obtained from all the far cells of C by using the L2L translation if $l > s$ or the H2H translation if $l \leq s$. However, as for a cell at level 2, the coefficients are obtained by the M2L or F2H translation only. In the downward pass, when $l = s$, the H2L conversion should be used to convert the local expansion coefficients of the high-frequency FMM to those of the low-frequency FMM.

4.4 Evaluation of the integrals

Now, evaluate the boundary integrals of all collocation points contained in a leaf cell C at level l. Firstly, calculate the contributions from all boundary elements in C and its adjacent cells directly as in the CBEM. Then, compute the contributions from all the other cells (cells in the interaction list and far cells of C) by shifting the local expansion coefficients from the center of C to the collocation points. If $l > s$, the low-frequency formulas should be used, otherwise, the high-frequency formulas should be employed. The summation of all these contributions gives the final value of boundary integrals.

In the case of calculating the matrix and known vector product on the right-hand side of Eq. 13, the above procedures can provide the final results. However, when calculating the matrix and unknown vector product on the left-hand side of Eq. 13, we need to update the unknown vector in the iterative solver, such as the GMRES in this paper, and then continue at 3.2 for the matrix-vector product until the solution converges within a given tolerance.

5 Numerical Examples

Numerical examples are employed in this section to show the accuracy and efficiency of the present algorithm for there dimensional acoustic shape sensitivity analyses. In all the examples presented below, we define the objective function as

follows:

$$J = \int_{\Omega} p(x)\delta(x-z)\,\mathrm{d}\Omega, \quad z \in \Omega \tag{59}$$

so that,

$$\dot{J} = \dot{p}(z) \tag{60}$$

In this case, the adjoint equation should be defined as

$$\nabla^2\lambda(x) + k^2\lambda(x) + \delta(x-z) = 0, \quad x,z \in \Omega \tag{61}$$

with the following boundary conditions:

$$\frac{\partial\lambda}{\partial n}(x) = 0, \quad x \in \Gamma_q \tag{62}$$

$$\lambda(x) = 0, \quad x \in \Gamma_u \tag{63}$$

The acoustic medium is assumed to be air with the density of $\rho = 1.2\,[\mathrm{kg/m^3}]$ and the sound speed of $c = 340.0\,[\mathrm{m/s}]$. Constant triangular elements are used to discretize the boundary surface, for instance as shown in Fig. 1. In the FMM algorithm, the maximum number of elements contained in a leaf cell is set to 100. The threshold D between the low- and high-frequency strategies is 0.2λ, where λ is the acoustic wavelength. The number of truncation terms is determined by the semi-empirical formula $p = kd^l + 5\ln(kd^l + \pi)$, where d^l is the edge length of the cells at level l [Song, Lu, and Chew (1997)]. The Gaussian quadrature formula with 10 integration points is used to evaluate all integrals numerically [Stroud and Secrest (1966)]. The GMRES solver stops iterations when the residue is below the tolerance of 10^{-3}. All the computations presented below were done on a desktop PC with an Intel 2.93GHz Core CPU and 4GB RAM.

5.1 Pulsating sphere example

A pulsating sphere of radius $a = 1.0\,[\mathrm{m}]$ is selected as the first example in this section. The analytical pressure sensitivity with respect to a radius change is given by

$$\frac{\partial u(r)}{\partial a} = \frac{\rho ckv_n}{r}\left\{\frac{\partial v_n}{\partial a}\frac{\mathrm{i}a}{1-\mathrm{i}ka} + v_n\left[\frac{2\mathrm{i}+ka}{1-\mathrm{i}ka} - \frac{ka}{(1-\mathrm{i}ka)^2}\right]\right\}\mathrm{e}^{\mathrm{i}k(r-a)} \tag{64}$$

where r is the distance from the center of the sphere to the field point of interest and v_n the uniform radial velocity on the surface.

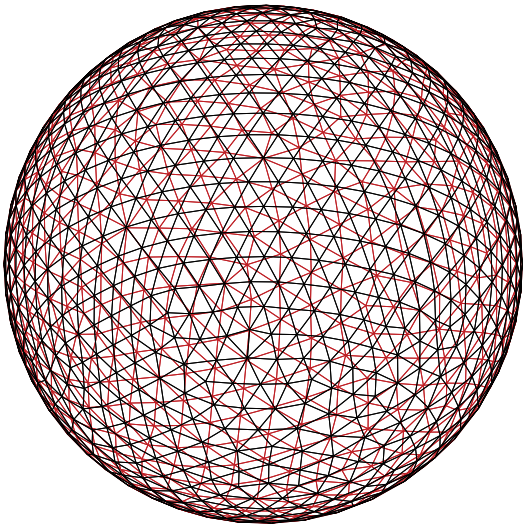

Figure 1: Mesh discretization of the sphere model (2044 triangular elements)

In the numerical analysis, the radial velocity v_n is set to $1.0\,[\mathrm{m/s}]$ and its sensitivity $\partial v_n/\partial a$ is set to $1.0\,[\mathrm{s}^{-1}]$. Sensitivities of sound pressure at a field point with $r = 6.0\,[\mathrm{m}]$ are calculated and compared with the analytical solutions for a wave number range from 0.5 to 5.0. The mesh discretization depicted in Fig. 1 is used to obtain the numerical results plotted in Figs. 2 and 3. Fig. 2 shows the comparison of the real part of the results, while Fig. 3 shows the comparison of their imaginary parts. It can be observed that the numerical results obtained by the present FMBEM sensitivity approach are very close to those obtained by the conventional method (CBEM) and also follow the analytical solutions very well. Since the Burton-Miller BIE formula is employed, the FMBEM sensitivity approach as well as the CBEM yields unique solutions over the wave number range.

5.2 Oscillating sphere example

Another sphere oscillating with a velocity v_z in the direction z is chosen as the second example in this section. The radius a is also designated as the design variable

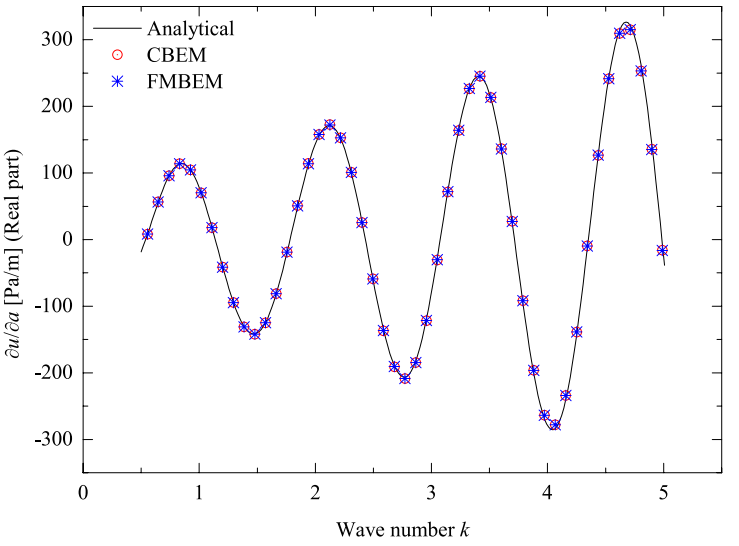

Figure 2: Comparison of the real part of the solutions of the pulsating sphere example

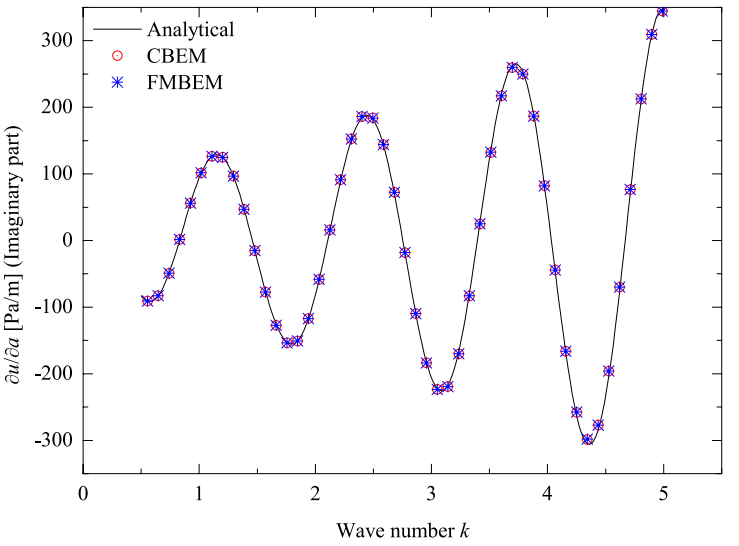

Figure 3: Comparison of the imaginary part of the solutions of the pulsating sphere example

and the analytical sensitivity of sound pressure is given as

$$\frac{\partial u(r,\theta)}{\partial a} = \frac{\mathrm{i}\rho ck a^2(1-\mathrm{i}kr)}{r^2}\left\{\frac{\partial v_z}{\partial a}\frac{a}{2-2\mathrm{i}ka-k^2a^2} + v_z\left[\frac{3-\mathrm{i}ka}{2-2\mathrm{i}ka-k^2a^2}+\frac{2\mathrm{i}ka(1-\mathrm{i}ka)}{(2-2\mathrm{i}ka-k^2a^2)^2}\right]\right\}\mathrm{e}^{\mathrm{i}k(r-a)}\cos\theta \tag{65}$$

where r is also the distance from the center of the sphere to the field point of interest and θ the inclination angle of the field point measured from the z direction.

In the numerical computation, the initial radius a is also set to 1.0 [m], the velocity $v_z = 1.0$ [m/s] and its sensitivity $\partial v_z/\partial a = 0$. Sound pressure sensitivities versus wave numbers from 0.5 to 5.0 are calculated at a field point with $r = 6.0$ [m] and $\theta = 0$. The mesh discretized model depicted in Fig. 1 is used to obtain the numerical results shown in Figs. 4 and 5, where we also observe that the present FMBEM sensitivity approach based on the Burton-Miller formula produces accurate results for the whole wave number range.

5.3 Convergence and efficiency studies

In the above two examples, it has been shown that the present sensitivity approach can provide very accurate solutions for exterior acoustic wave problems. In this subsection, we analyze the convergence behavior to further verify the present approach. Also, the computational times are compared so as to demonstrate the efficiency of the present sensitivity approach. Again, the pulsating sphere example used in the first example is employed in this subsection. In the numerical calculation, the wave number k is set to be 5.0, the sample field point is taken at $r = 6.0$ [m].

Fig. 6 shows the comparisons of relative errors between the conventional BEM sensitivity approaches and the present one based on the FMBEM approach. We refer to CBEM-LU and CBEM-GMRES as the results obtained by CBEM with LU-decomposition method and GMRES solvers, respectively; and FMBEM as those obtained by the present wideband fast multipole boundary element sensitivity approach. As demonstrated in Fig. 6, the percentage relative errors of the CBEM-LU, CBEM-GMRES and FMBEM results are very close to each other and decrease very fast as the element number increases. The computational efficiencies of the present fast sensitivity algorithm as compared with the conventional BEM sensitivity approaches are shown in Fig. 7. It is observed that the present sensitivity approach is faster than the CBEM-LU for models with more than 2000 elements, and also faster than the CBEM-GMRES for models with more than 8000 elements in this study. So that, the present fast sensitivity approach is found to be very powerful for large-scale problems.

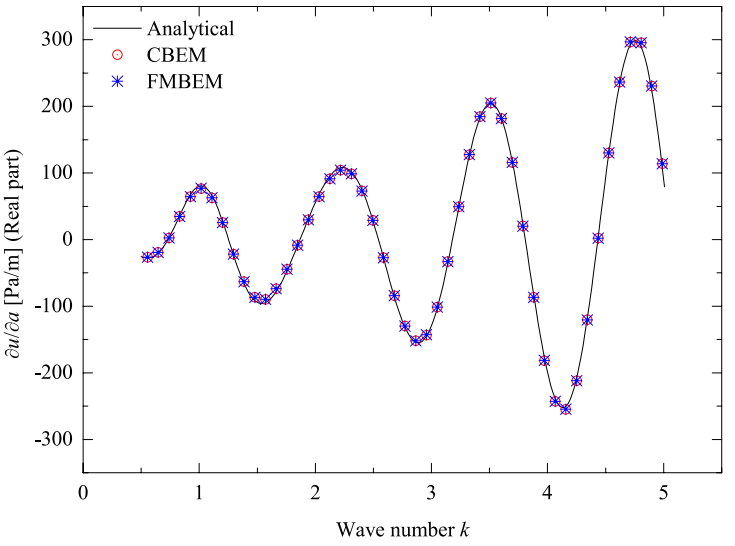

Figure 4: Comparison of the real part of the solutions of the oscillating sphere example

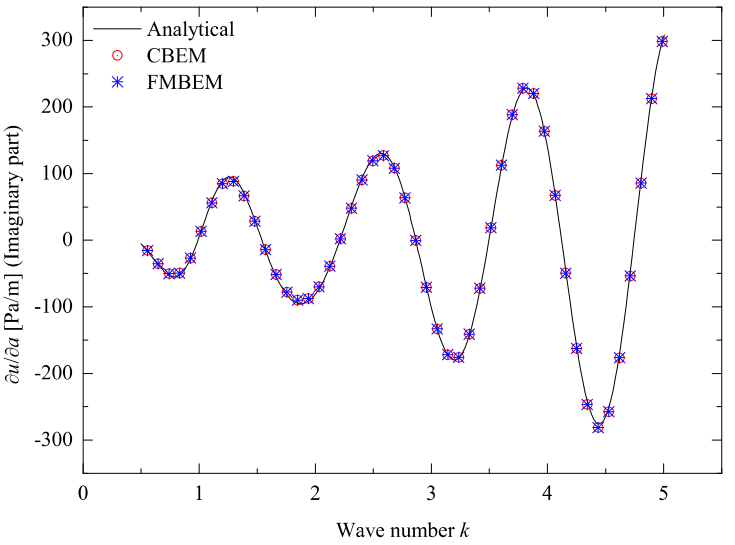

Figure 5: Comparison of the imaginary part of the solutions of the oscillating sphere example

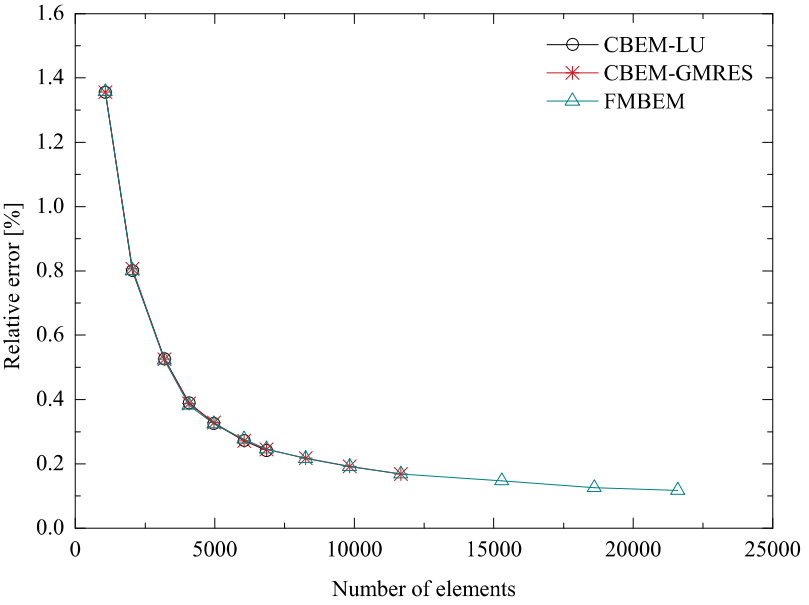

Figure 6: Relative errors of the solutions of the pulsating sphere example

6 Conclusions

A 3-D acoustic shape sensitivity analysis algorithm by means of the adjoint variable method and the wideband FMBEM approach is proposed in this paper. The sensitivity equation is obtained by the adjoint variable method with the concept of material derivative. The governing PDEs are solved using a Burton-Miller BIE formula so as to conquer the non-uniqueness problem of the conventional boundary integral equation method when solving exterior acoustic wave problems. The wideband FMM and the GMRES solver are employed to accelerate the computations. Numerical examples clearly demonstrate the potential of the present approach for solving large-scale acoustic shape sensitivity problems.

Since the adjoint variable method is adopted, the computational time depends on the number of objective functions rather than the number of design variables as in the direct differentiation method. The adjoint equation is derived in a continuous form so that we avoid calculating the sensitivities of the coefficient matrices, which are still not easy to obtain in the discrete adjoint variable method [Kim and Dong (2006)]. In the numerical analysis, because the constant element is used to dis-

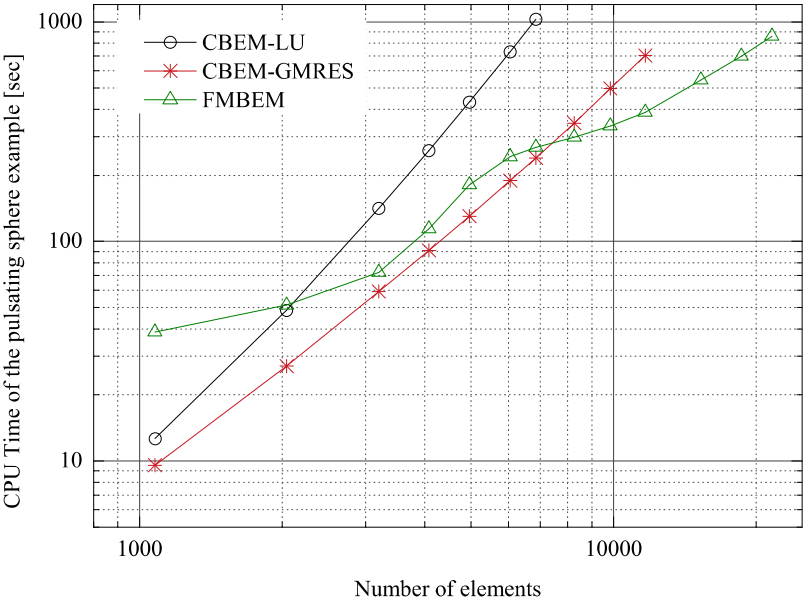

Figure 7: CPU time used to solve the pulsating sphere example

cretize the boundary, the strongly- and hyper-singular boundary integrals existing in the formulas can be evaluated explicitly and directly. Therefore, no additional multipole expansion formulas, which are needed in the FMBEM approach based on the regularized boundary integral representations, are required in the present formulation.

Further studies can be carried out for more complicated and practical engineering problems by the developed algorithm. Although, this paper is focused only on the acoustic problems, the approach can also be applied to solve other types of sensitivity problems, such as potential, elastostatic and elastodynamic problems.

Acknowledgement: C.J. Zheng would like to thank the China Scholarship Council (CSC) and Nagoya University for the financial support of the study in Nagoya University of Japan. T. Matsumoto acknowledges the financial support by "Development of fast and large-scale acoustic design sensitivity analysis system by means of BEM", Adaptable and Seamless Technology Transfer Program through Target-driven R&D, JST. Financial support from the National Nature Science Foundation of China under Grant no. 11172291 is also acknowledged.

References

Abramowitz, M.; Stegun, I. (1972): *Handbook of mathematical functions with formulas, graphs, and mathematical tables*. Dover, New York.

Amini, S.; Harris, P. (1990): A comparison between various boundary integral formulations of the exterior acoustic problem. *Comput. Method. Appl. M.*, vol. 84, pp. 59–75.

Arai, Y.; Tanaka, M.; Matsumoto, T. (2007): A new boundary element analysis of 3-D acoustic fields avoiding the fictitious eigenfrequency problem. *Trans. JSME C.*, vol. 73, no. 729, pp. 112–119.

Arai, Y.; Tanaka, M.; Matsumoto, T. (2007): A new design sensitivity analysis of acoustic problems based on bem avoiding fictitious eigenfrequency issue. *Trans. JSME C.*, vol. 73, no. 729, pp. 120–127.

Arora, J. (1993): An exposition of the material derivative approach for structural shape sensitivity analysis. *Comput. Method. Appl. M.*, vol. 105, pp. 41–62.

Beylkin, G.; Coifman, R.; Rokhlin, V. (1991): Fast wavelet transforms and numerical algorithms I. *Commun. Pure Appl. Math.*, vol. 44, pp. 141–183.

Brebbia, C.; Dominguez, J. (1989): *Boundary elements- an introductory course*. McGraw Hill, New York.

Burczyński, T.; Kane, J.; Balakrishna, C. (1995): Shape design sensitivity analysis via material derivative-adjoint variable technique for 3-D and 2-D curved boundary elements. *Int. J. Numer. Meth. Eng.*, vol. 38, pp. 2839–2866.

Burton, A.; Miller, G. (1971): The application of integral equation methods to the numerical solution of some exterior boundary-value problems. *Proc. Roy. Soc. Lond. A.*, vol. 323, pp. 201–210.

Chen, H.; Fu, D.; Zhang, P. (2007): An investigation of wave propagation with high wave numbers via the regularized LBIEM. *CMES: Computer Modeling in Engineering & Sciences*, vol. 20, no. 2, pp. 85–98.

Cheng, H.; Crutchfield, W.; Gimbutas, Z.; Greengard, L.; Ethridge, J.; Huang, J.; Rokhlin, V.; Yarvin, N.; Zhao, J. (2006): A wideband fast multipole method for the Helmholtz equation in three dimensions. *J. Comput. Phys.*, vol. 216, pp. 300–325.

Cheng, H.; Greengard, L.; Rokhlin, V. (1999): A fast adaptive multipole algorithm in three dimensions. *J. Comput. Phys.*, vol. 155, pp. 468–498.

Chien, C.; Rajiyah, H.; Atluri, S. (1990): An effective method for solving the hypersingular integral equations in 3-D acoustics. *J. Acoust. Soc. Am.*, vol. 88, no. 2, pp. 918–937.

Cipra, B. (2000): The Best of the 20th Century: Editors Name Top 10 Algorithms. *SIAM News*, vol. 33.

Ciskowski, R.; Brebbia, C. (1991): *Boundary elment methods in acoustics*. Computational Mechanics Publications, Southampton.

Coifman, R.; Rokhlin, V.; Wandzura, S. (1993): The fast multipole method for the wave equation: a pedestrian prescription. *IEEE Antennas Propag. Mag.*, vol. 35, no. 3, pp. 7–12.

Darve, E.; Havé, P. (2004): A fast multipole method for Maxwell equations stable at all frequencies. *Phil. Trans. R. Soc. Lond. A*, vol. 362, pp. 603–628.

Epton, M.; Dembart, B. (1995): Multipole translation theory for the three dimensional Laplace and Helmholtz equations. *SIAM J. Sci. Comput.*, vol. 16, pp. 865–897.

Greengard, L.; Rokhlin, V. (1987): A fast algorithm for particle simulations. *J. Comput. Phys.*, vol. 73, pp. 325–348.

Greengard, L.; Rokhlin, V. (1997): A new version of the fast multipole method for the Laplace equation in three dimensions. *Acta Numerica*, pp. 229–269.

Gumerov, N.; Duraiswami, R. (2009): A broadband fast multipole accelerated boundary element method for the three dimensional Helmholtz equation. *J. Acoust. Soc. Am.*, vol. 125, no. 1, pp. 191–205.

Gyure, M.; Stalzer, M. (1998): A prescription for the multilevel Helmholtz FMM. *IEEE Comput. Sci. Eng.*, pp. 39–47.

Hackbusch, W. (1999): A sparse matrix arithmetic based on H-matrices, part 1: introduction to H-matrices. *Comput.*, vol. 62, pp. 89–108.

Haug, E.; Choi, K.; Komkov, V. (1986): *Design sensitivity analysis of structural systems*. Academic Press Inc, New York.

Hwang, W. (1997): Hypersingular boundary integral equations for exterior acoustic problems. *J. Acoust. Soc. Am.*, vol. 101, no. 6, pp. 3336–3342.

Kim, N.; Dong, J. (2006): Shape sensitivity analysis of sequential structural-acoustic problems using FEM and BEM. *J. Sound Vib.*, vol. 290, pp. 192–208.

Koo, B.; Ih, J.; Lee, B. (1998): Acoustic shape sensitivity analysis using the boundary integral equation. *J. Acoust. Soc. Am.*, vol. 104, no. 5, pp. 2851–2860.

Kress, R. (1985): Minimizing the condition number of boundary integral operators in acoustic and electromagnetic scattering. *Q. J. Mech. Appl. Math.*, vol. 38, pp. 323–343.

Li, S.; Huang, Q. (2010): An improved form of the hypersingular boundary integral equation for exterior acoustic problems. *Eng. Anal. Boundary Elem.*, vol. 34, pp. 189–195.

Liu, Y.; Rizzo, F. (1992): A weakly singular form of the hypersingular boundary integral equation applied to 3-D acoustic wave problems. *Comput. Meth. Appl. Mech. Eng.*, vol. 96, pp. 271–287.

Matsumoto, T.; Tanaka, M.; Yamada, Y. (1995): Design sensitivity analysis of steady-state acoustic problems using boundary integral equation formulation. *JSME Int. J. C.*, vol. 38, no. 1, pp. 9–16.

Matsumoto, T.; Zheng, C.; Harada, S.; Takahashi, T. (2010): Explicit evaluation of hypersingular boundary integral equation for 3-D Helmholtz equation discretized with constant triangular element. *J. Comput. Sci. Eng.*, vol. 4, no. 3, pp. 194–206.

Nishimura, N. (2002): Fast multipole accelerated boundary integral equation methods. *ASME Appl. Mech. Rev.*, vol. 55, no. 4, pp. 299–324.

Nowak, A. (1989): The multiple reciprocity method of solving heat conduction problems. *Proceedings of the 11th International Conference on Boundary Element Methods*, vol. 2, pp. 81–95.

Otani, Y.; Nishimura, N. (2008): A periodic FMM for Maxwell's equations in 3D and its applications to problems related to photonic crystals. *J. Comput. Phys.*, vol. 227, pp. 4630–4652.

Partridge, P.; Brebbia, C.; Wrobel, L. (1991): *The dual reciprocity boundary element method*. Computational Mechanics Publications, Southampton.

Phillips, J.; White, J. (1997): A precorrected-FFT method for electrostatic analysis of complicated 3-D structures. *IEEE Trans. Comput. Aided Des. Integr. Circuits Syst.*, vol. 16, pp. 1059–1072.

Qian, Z.; Han, Z.; Atluri, S. (2004): Directly derived non-hyper-singular boundary integral equations for acoustic problems, and their solution through Petrov-Galerkin Schemes. *CMES: Computer Modeling in Engineering & Sciences*, vol. 5, no. 6, pp. 541–562.

Qian, Z.; Han, Z.; Ufimtsev, P.; Atluri, S. (2004): Non-hypersingular boundary integral equations for acoustic problems, implemented by the collocation-based boundary element method. *CMES: Computer Modeling in Engineering & Sciences*, vol. 6, no. 2, pp. 133–144.

Rahola, J. (1996): Diagonal forms of the translation operators in the fast multipole algorithm for scattering problems. *BIT*, vol. 36, no. 2, pp. 333–358.

Rokhlin, V. (1993): Diagonal forms of translatioin operators for the Helmholtz equation in three dimensions. *Appl. Comput. Harmon. Anal.*, vol. 1, pp. 82–93.

Saad, Y.; Schultz, M. (1986): GMRES: A generalized minimal residual algorithm for solving nonsymmetric linear systems. *SIAM J. Sci. Stat. Comput.*, vol. 7, no. 3, pp. 856–869.

Schenck, H. (1968): Improved integral formulation for acoustic radiation problems. *J. Acoust. Soc. Am.*, vol. 44, pp. 41–58.

Shen, L.; Liu, Y. (2007): An adaptive fast multipole boundary element method for three-dimensional acoustic wave problems based on the Burton-Miller formulations. *Comput. Mech.*, vol. 40, pp. 461–472.

Shen, L.; Liu, Y. (2007): An adaptive fast multipole boundary element method for three-dimensional potential problems. *Comput. Mech.*, vol. 39, pp. 681–691.

Smith, D.; Bernhard, R. (1992): Computation of acoustic shape design sensitivity using a boundary element method. *J. Vib. Acoust.*, vol. 114, pp. 127–132.

Sommerfeld, A. (1949): *Partial Differential Equations in Physics*. Academic Press Inc, New York.

Song, J.; Lu, C.; Chew, W. (1997): Multilevel fast multipole algorithm for Electromagnetic scattering by large complex objects. *IEEE Trans. Antennas Propag.*, vol. 45, no. 10, pp. 1488–1493.

Stroud, A.; Secrest, D. (1966): *Gaussian Quadrature Formulas*. Englewood Cliffs, NJ: Prentice-Hall.

Tanaka, M.; Sladek, V.; Sladek, J. (1994): Regularization techniques applied to boundary element methods. *ASME Appl. Mech. Rev.*, vol. 47, no. 10, pp. 457–499.

Udawalpola, R. (2010): *Shape optimization for acoustic wave propagation problems*. PhD Thesis, Uppsala University, Uppsala, Sweden.

Udawalpola, R.; Wadbro, E.; Berggren, M. (2011): Optimization of a variable mouth acoustic horn. *Int. J. Numer. Meth. Eng.*, vol. 85, pp. 591–606.

Wolf, W.; Lele, S. (2010): Wideband fast multipole boundary element method: Application to acoustic scattering from aerodynamic bodies. *J. Numer. Meth. Fluids*.

Yan, Z.; Hung, K.; Zheng, H. (2003): Solving the hypersingular boundary integral equation in three-dimensional acoustic using a regularization relationship. *J. Acoust. Soc. Am.*, vol. 113, no. 5, pp. 2674–2683.

Yoshida, K. (2001): *Applications of fast multipole method to boundary integral equation method*. PhD Thesis, Kyoto University, Kyoto, Japan.

Yoshida, K.; Nishimura, N.; Kobayashi, S. (2001): Application of new fast multipole boundary integral equation method to crack problems in 3D. *Eng. Anal. Boundary Elem.*, vol. 25, pp. 239–247.

Zhang, Y.; Bi, C.; Chen, J.; Chen, X. (2009): Adjoint variable method for structural-acoustic sensitivity analysis based on wave superposition. *Chinese Journal of Mechanical Engineering*, vol. 45, no. 4, pp. 177–182.

Appendix A: Material derivative of $\hat{J}$

The function $\hat{J}$ is constituted of the original objective function J and the constraint condition R. As the material derivative of J has already been given as Eq. 16, we only need to calculate the material derivative of R in the following. According to Green's first identity, we have

$$R = \int_\Gamma \lambda(x) q(x)\,\mathrm{d}\Gamma - \int_\Omega \lambda_{,i}(x) u_{,i}(x)\,\mathrm{d}\Omega + \int_\Omega k^2 \lambda(x) u(x)\,\mathrm{d}\Omega \tag{66}$$

Then, the material derivatives of the three terms of R can easily be obtained as follows:

$$\dot{R}_1 = \int_\Gamma \dot{\lambda}(x) q(x)\,\mathrm{d}\Gamma + \int_\Gamma \lambda(x) \dot{q}(x)\,\mathrm{d}\Gamma + \int_\Gamma \lambda(x) q(x)\,\mathrm{d}\dot{\Gamma} \tag{67}$$

$$\begin{aligned}\dot{R}_2 = &\int_\Omega \dot{\lambda}_{,i}(x) u_{,i}(x)\,\mathrm{d}\Omega - \int_\Omega \lambda_{,j}(x) u_{,i}(x) \dot{x}_{j,i}\,\mathrm{d}\Omega \\ &+ \int_\Omega \lambda_{,i}(x) \dot{u}_{,i}(x)\,\mathrm{d}\Omega - \int_\Omega \lambda_{,i}(x) u_{,j}(x) \dot{x}_{j,i}\,\mathrm{d}\Omega + \int_\Omega \lambda_{,i}(x) u_{,i}(x) \dot{x}_{j,j}\,\mathrm{d}\Omega\end{aligned} \tag{68}$$

$$\dot{R}_3 = \int_\Omega \left[k^2 \dot{\lambda}(x) u(x) + k^2 \lambda(x) \dot{u}(x) + k^2 \lambda(x) u(x) \dot{x}_{j,j} \right] \mathrm{d}\Omega \tag{69}$$

where we used Eq. 18 and the following equations prescribed in [Haug, Choi, and Komkov (1986); Arora (1993)]:

$$\dot{(\lambda_{,i}(x))} = \dot{\lambda}_{,i}(x) - \lambda_{,j}(x) \dot{x}_{j,i} \tag{70}$$

$$\dot{(u_{,i}(x))} = \dot{u}_{,i}(x) - u_{,j}(x) \dot{x}_{j,i} \tag{71}$$

According to Green's first identity again, we have

$$\int_\Omega \dot{\lambda}_{,i}(x) u_{,i}(x)\,\mathrm{d}\Omega = \int_\Gamma \dot{\lambda}(x) q(x)\,\mathrm{d}\Gamma - \int_\Omega \dot{\lambda}(x) u_{,ii}(x)\,\mathrm{d}\Omega \tag{72}$$

$$\int_\Omega \lambda_{,i}(x)\dot{u}_{,i}(x)\,\mathrm{d}\Omega = \int_\Gamma \frac{\partial \lambda}{\partial n}(x)\dot{u}(x)\,\mathrm{d}\Gamma - \int_\Omega \lambda_{,ii}(x)\dot{u}(x)\,\mathrm{d}\Omega \tag{73}$$

Substituting Eqs. 72 and 73 into Eq. 68, then adding $\dot{R}_1$, $\dot{R}_2$ and $\dot{R}_3$ together, we obtain

$$\begin{aligned}\dot{R} = &\int_\Gamma \lambda(x)\dot{q}(x)\,\mathrm{d}\Gamma - \int_\Gamma \frac{\partial \lambda}{\partial n}(x)\dot{u}(x)\,\mathrm{d}\Gamma + \int_\Gamma \lambda(x)q(x)\,\mathrm{d}\dot{\Gamma} \\ &+ \int_\Omega \Big\{ [\lambda_{,ii}(x) + k^2\lambda(x)]\dot{u}(x) + [u_{,ii}(x) + k^2 u(x)]\dot{\lambda}(x) \\ &+ \lambda_{,j}(x)u_{,i}(x)\dot{x}_{j,i} + \lambda_{,i}(x)u_{,j}\dot{x}_{j,i} - \lambda_{,i}(x)u_{,i}(x)\dot{x}_{j,j} + k^2\lambda(x)u(x)\dot{x}_{j,j} \Big\}\,\mathrm{d}\Omega \end{aligned} \tag{74}$$

Moreover, we have

$$\begin{aligned}\lambda_{,j}u_{,i}\dot{x}_{j,i} + \lambda_{,i}u_{,j}\dot{x}_{j,i} - \lambda_{,i}u_{,i}\dot{x}_{j,j} = &(\lambda_{,j}u_{,i}\dot{x}_j)_{,i} + (\lambda_{,i}u_{,j}\dot{x}_j)_{,i} \\ &- (\lambda_{,i}u_{,i}\dot{x}_j)_{,j} - \lambda_{,ii}u_{,j}\dot{x}_j - \lambda_{,j}u_{,ii}\dot{x}_j \end{aligned} \tag{75}$$

According to the divergence theorem, we obtain

$$\begin{aligned}\int_\Omega \left(\lambda_{,j}u_{,i}\dot{x}_{j,i} + \lambda_{,i}u_{,j}\dot{x}_{j,i} - \lambda_{,i}u_{,i}\dot{x}_{j,j}\right)\mathrm{d}\Omega = &\int_\Gamma (\lambda_{,j}u_{,i}n_i + \lambda_{,i}u_{,j}n_i - \lambda_{,i}u_{,i}n_j)\dot{x}_j\,\mathrm{d}\Gamma \\ &- \int_\Omega (\lambda_{,ii}u_{,j} + \lambda_{,j}u_{,ii})\dot{x}_j\,\mathrm{d}\Omega \end{aligned} \tag{76}$$

also, we have

$$\int_\Omega k^2[\lambda u_{,j}\dot{x}_j + \lambda_{,j}u\dot{x}_j + \lambda u\dot{x}_{j,j}]\mathrm{d}\Omega = \int_\Gamma k^2\lambda u\dot{x}_j n_j\,\mathrm{d}\Gamma \tag{77}$$

Substituting Eqs. 76 and 77 into Eq. 74, and considering that $\nabla^2 u(x) + k^2 u(x) = 0$ should be satisfied within the domain, we obtain

$$\begin{aligned}\dot{R} = &\int_\Gamma \lambda(x)\dot{q}(x)\,\mathrm{d}\Gamma - \int_\Gamma \frac{\partial \lambda}{\partial n}(x)\dot{u}(x)\,\mathrm{d}\Gamma + \int_\Gamma \lambda(x)q(x)\,\mathrm{d}\dot{\Gamma} \\ &+ \int_\Omega [\lambda_{,ii}(x) + k^2\lambda(x)]\dot{u}(x)\,\mathrm{d}\Omega - \int_\Omega [\lambda_{,ii}(x) + k^2\lambda(x)]u_{,j}(x)\dot{x}_j\,\mathrm{d}\Omega \\ &+ \int_\Gamma \left(\lambda_{,j}q + \frac{\partial \lambda}{\partial n}u_{,j} - \lambda_{,i}u_{,i}n_j + k^2\lambda u n_j\right)\dot{x}_j\,\mathrm{d}\Gamma \end{aligned} \tag{78}$$

Finally, the material derivative of $\hat{J}$ can be written as

$$\begin{aligned}\dot{\hat{J}} &= \int_\Gamma \left(\frac{\partial g}{\partial u} - \frac{\partial \lambda}{\partial n}\right)\dot{u}\,\mathrm{d}\Gamma + \int_\Gamma \left(\frac{\partial g}{\partial q} + \lambda\right)\dot{q}\,\mathrm{d}\Gamma \\ &+ \int_\Gamma \left(\lambda_{,j} q + \frac{\partial \lambda}{\partial n} u_{,j} - \lambda_{,i} u_{,i} n_j + k^2 \lambda u n_j\right)\dot{x}_j\,\mathrm{d}\Gamma \\ &+ \int_\Gamma (g(u,q) + \lambda q)\,\mathrm{d}\dot{\Gamma} + \int_\Omega \left(\lambda_{,ii} + k^2\lambda + \frac{\partial h}{\partial u}\right)\dot{u}\,\mathrm{d}\Omega \\ &- \int_\Omega (\lambda_{,ii} + k^2\lambda) u_{,j}\dot{x}_j\,\mathrm{d}\Omega + \int_\Omega h(u)\,\mathrm{d}\dot{\Omega} \end{aligned} \tag{79}$$